Sb complexes and Zn interstitials in Sb-implanted ZnO epitaxial films*

Liu Yao-Ping(刘尧平)[a], Ying Min-Ju(英敏菊)[b], Mei Zeng-Xia(梅增霞)[a], Li Jun-Qiang(李俊强)[a], Du Xiao-Long(杜小龙)[a]†, and A. Yu. Kuznetsov[c]‡

[a] *Beijing National Laboratory for Condensed Matter Physics, Institute of Physics, Chinese Academy of Sciences, Beijing* 100190, *China*

[b] *College of Nuclear Science and Technology, Beijing Normal University, Beijing* 100875, *China*

[c] *Department of Physics, University of Oslo, P.O. Box* 1048 *Blindern, NO*-0316 *Oslo, Norway*

(Received 3 December 2010; revised manuscript received 18 January 2011)

In the present work, post-annealing is adopted to investigate the formation and the correlation of Sb complexes and Zn interstitials in Sb-ion implanted ZnO films, by using Raman scattering technique and electrical characterizations. The damage of Zn sublattice, produced by ion bombardment process is discerned from the unrecovered E_2 (L) peak in annealed high Sb^+ dose implanted samples. It is suggested that the Zn sublattice may be strongly affected by the introduction of Sb dopant because of the formation of Sb_{Zn}–$2V_{Zn}$ complex acceptor. The appearance of a new peak at 510 cm^{-1} in the annealed high dose Sb^+ implanted samples is speculated to result from (Zn interstitials-O interstitials) Zn_i–O_i complex, which is in a good accordance with the electrical measurement. The p-type ZnO is difficult to obtain from the Sb^+ implantation, however, which can be realized by *in-situ* Sb doping with proper growth conditions instead.

Keywords: ZnO, ion implantation, Raman spectra, molecular beam epitaxy

PACS: 61.72.U–, 61.72.uj, 78.30.–j, 81.15.Hi **DOI:** 10.1088/1674-1056/20/6/066104

1. Introduction

As an important wide bandgap semiconductor (E_g = 3.37 eV) with large exciton binding energy (60 meV), ZnO has been studied extensively due to its potential applications in next-generation short-wavelength optoelectronic devices, such as light emitting diodes (LEDs) and laser diodes (LDs).[1–3] However, a formidable challenging issue, namely the growth of reliable and repeatable p-type ZnO materials, has severely hampered the progress in its optoelectronic device applications. Many groups have presented their work on p-ZnO fabrication with different dopants, Li or N for example, substituting Zn or O matrix atoms and generating extrinsic holes.[4,5] On the other hand, there has been no effective method of preparing stable and reproducible p-ZnO materials until now. It is received that either some dopant-induced defects such as Li interstitial, or native defects such as Zn interstitial (Zn_i) and oxygen vacancy (V_O), will result in a strong self-compensation effect and make it difficult to realize p-type conductivity in ZnO.[6,7] In the case of doping with group-V elements, like As and Sb to replace O, theoretical studies indicate that their energy levels are located deeply in the band gap of ZnO and are unlikely to be ionized at room temperature.[8]

Some groups have reported their results about the realization of p-ZnO by Sb doping as well as the fabrication of homo-junction diodes.[9,10] However, the issue of possible compensation effects associated with Sb induced defects has not been well understood yet. An interesting microscopic configuration for Sb and As sites in ZnO was proposed by Limpijumnong *et al.*[11] based on the density functional calculations, where As or Sb atoms occupy Zn site (As_{Zn} and Sb_{Zn}) instead of O site and form complex acceptors with two Zn vacancies (V_{Zn}) (As_{Zn}–$2V_{Zn}$ or Sb_{Zn}–$2V_{Zn}$). The above-mentioned hypothesis has not been experimentally confirmed yet, though it is very important for the understanding of the compensation effect in p-ZnO dop-

*Project supported by the National Natural Science Foundation of China (Grant Nos. 61076007 and 50532090), the National Basic Research Program of China (Grant Nos. 2007CB936203, 2009CB929400, 2009AA033101, and 2011CB302002), the Knowledge Innovation Project of the Chinese Academy of Sciences, and the Research Council of Norway through the FRINAT "Understanding ZnO" Project.

†Corresponding author. E-mail: xldu@aphy.iphy.ac.cn

‡Corresponding author. E-mail: andrej.kuznetsov@fys.uio.no

© 2011 Chinese Physical Society and IOP Publishing Ltd

ing. Ion implantation would be a convincing method to investigate the mechanism of Sb doping in ZnO, for the ion implanting process introduces large lattice disorder and various defects, which may be recovered by annealing at high temperature. The ion-implantation doping is also a possible approach to achieving the p-type conductivity in ZnO at present.[12−14] To address these issues, Raman scattering technique, a nondestructive but strain-sensitive research method, is applied with a combination of post annealing to study the occupation sites of the dopant, the evolution of dopant induced defects and the lattice disorder in our work. Here, undoped ZnO thin films are synthesized by radio-frequency plasma assisted molecular beam epitaxy (rf-MBE) and then implanted with different dose Sb^+ ions. It should be noted that the influence of some unintentional-doped impurities, such as Li, Na, K, etc. in bulk ZnO single crystal grown by hydrothermal method, can be absolutely excluded in our case.

2. Experiment

Single crystal ZnO (0001) thin films were grown on sapphire substrates under oxygen rich condition by rf-MBE with MgO buffer as reported in our previous study.[15] Elemental Zn (7N) was evapourated by Knudsen cells (Veeco) and radical oxygen (5N5) generated by rf-plasma system (SVTA) was used as radical source for the growth. The thickness of the thin film is about 850 nm and the electrical measurements confirm that the as-grown ZnO thin film has an n-type conductivity and the carrier concentration, the mobility and the resistivity are $\sim 2 \times 10^{16}$ cm^{-3}, $\sim$ 20 cm^2/V$\cdot$s, and $\sim$ 15 $\Omega\cdot$cm, respectively. Then the ZnO film was cut into several pieces and 550-keV Sb^+ ions were homogeneously implanted in a dose range from 1×10^{12} ions/cm^2 to 1×10^{15} ions/cm^2 at room temperature. In order to discriminate the influence of radiation defects from that of Sb-induced defects, a controlled experiment of implanting similarly heavy Xe^+ ions with the same dose was performed on the same undoped ZnO films. After that, all the as-implanted samples were cut into two parts and one of them was annealed at 800 °C for 20 min in MBE chamber under oxygen plasma protection. The X-ray diffraction (XRD) spectra revealed that all the ZnO thin films were single crystal and no new peak was detected in the annealed samples (not shown here). These observations indicated that there was no new phase formed in the implanted ZnO samples both before and after anneal. The Raman measurements were carried out using an LabRam HR-800 system with an Nd: YAG laser (532 nm) as an excitation source at room temperature. The laser beam was focused by a microscope objective yielding a spot size of 1 μm. The scattered light was detected in backscattering geometry and recorded with a liquid nitrogen-cooled charge coupled device detector. The electrical properties were characterized by van der Pauw method in a home-made hall measurement system (EMO 600, IPCAS),[16] which was specially designed to trace the hall voltage during measurements so as to exclude the influence of persistent photoconductivity of ZnO film. Thus, the conductivity type and electrical parameters such as carrier concentration, mobility, etc., can be determined reliably.[16]

3. Results and discussion

There are several prominent peaks in the as-grown samples observed in Fig. 1 and labeled with E_2 (L) at $\sim$ 101 cm^{-1}, $2E_2$ (M) at $\sim$ 337 cm^{-1} and E_2 (H) at $\sim$437 cm^{-1}. In addition, peaks related to signal characteristic for the α-Al_2O_3 substrate are labeled as "Sub". The intensities of all prominent peaks decrease with ion implantation dose increasing as clearly seen in Fig. 1 and inserts (a) and (b) show the details of E_2 (L) and E_2 (H). The decrease in the intensity of

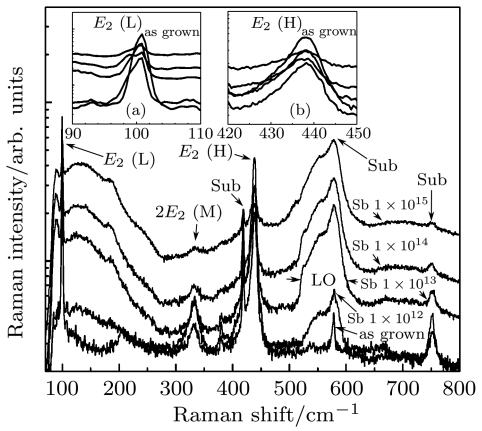


Fig. 1. Raman spectra of undoped and implanted ZnO by different Sb^+ doses. The inserts (a) and (b) show the intensity details of E_2 (L) and E_2 (H).

these prominent labeled peaks correlates nicely with the increase of radiation damage. Based on the previous identification in the literature, we attribute E_2 (L) and E_2 (H) to the vibrations involving in zinc and oxygen sublattices, respectively.[17] In contrast, broad modes around 520 cm^{-1}–580 cm^{-1} emerge, which is

commonly observed in the Raman spectra of the ion-implanted ZnO. The same signature of the Raman modes around 520 cm^{-1}–580 cm^{-1} was also observed in ZnO epitaxial films with Sb^+ implantations of different doses,[18] which were attributed to the disorder-active LO phonons.[19,20]

Figure 2 shows portions related to the E_2 (L), E_2 (H), and LO signatures in the Raman spectra of the annealed Sb^+ implanted ZnO, which are shown in panels (a), (b), and (c), respectively. Interestingly, the intensity of the E_2 (H) peak completely returned to the original value after annealing (see Fig. 2(b)) in all samples. These

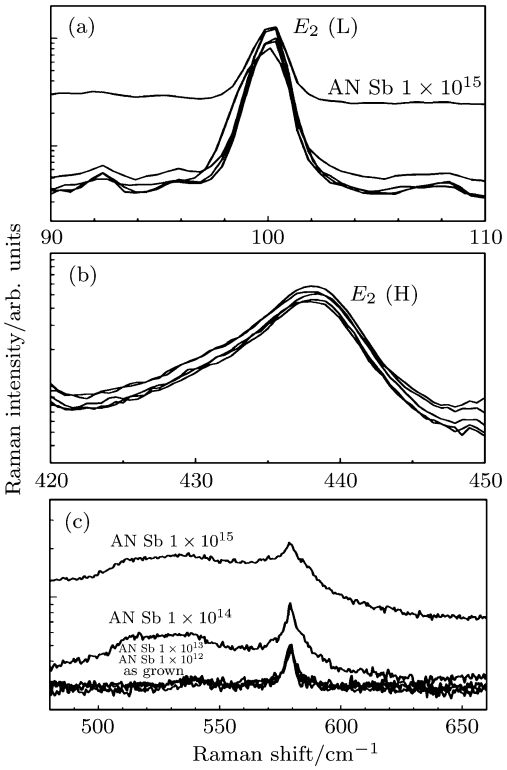


Fig. 2. Raman spectra of Sb^+ implanted ZnO after annealing and undoped ZnO relevant to E_2 (L) (a), E_2 (H) (b), and LO signatures (c).

evolutions confirm that the oxygen sublattice is fully recovered as a result of annealing in oxygen plasma environment where oxygen radicals specifically contribute to the modification of damaged oxygen sublattice (such as V_O). On the other hand, the Zn sublattice is found not to be fully recovered especially in high dose implanted samples (see Fig. 2(a)). One possible explanation for this discrepancy is that Sb atoms occupy Zn sites and probably form Sb_{Zn}–$2V_{Zn}$ complex after anneal, which was suggested and predicated to be an acceptor.[9] Formation of the Sb_{Zn}–$2V_{Zn}$ complex can prevent Zn_i, generated by ion implantation from diffusing back into the Zn sites during anneals. If the above mentioned scenario holds and accounts for the number of V_{Zn} needed to form Sb_{Zn}–$2V_{Zn}$ complex, we may anticipate high concentration of Zn_i in the Sb^+ implanted samples after annealing. However, the oxygen interstitial (O_i) can diffuse back to the oxygen site independent of the presence of Sb or complex forming at Zn sites. In Fig. 2(c), the distinct broad modes at 520 cm^{-1}–580 cm^{-1} disappear in the annealed samples with implantation doses of 1×10^{12} ions/cm^2 and 1×10^{13} ions/cm^2. Instead of the modes at 520 cm^{-1}–580 cm^{-1}, two peaks around 510 cm^{-1} and 536 cm^{-1} appear in the samples with the doses of 1×10^{14} ions/cm^2 and 1×10^{15} ions/cm^2, where the 536 cm^{-1} mode was also observed in the annealed lower dose implanted samples and the as-grown ZnO. Note that the $\sim$ 536 cm^{-1} mode also occurs for pure ZnO, Cusco *et al.*[21] ascribed the mode at 536 cm^{-1} to the 2× LA process. Importantly, we attribute the 510 cm^{-1} mode to the defects introduced by Sb^+ implantation in accordance with the argument given below.

Figure 3 shows the Raman spectra of annealed Xe^+ implanted ZnO, where signatures related to the E_2 (L), E_2 (H), and LO are shown in panels (a), (b), and (c), respectively. Note, the evolution of the prominent peaks as labeled E_2 (L), E_2 (H), and LO in Fig. 1 demonstrate the same trends in Xe^+ implanted samples (not shown here). It indicates that the implanted Xe^+ can introduce the same defects in ZnO films by ion bombardment as the implanted Sb^+ because of their similar ion size. However, the annealing process results in a full recovery of both Zn and O sublattice as confirmed by the observations in Figs. 3(a) and 3(b), respectively. Our interpretation of this fact is straightforward—Xe^+, in contrast with Sb^+, has no tendency to be incorporated on either Zn or O sites correlating with E_2 (L) and E_2 (H). Moreover, there is no peak appearing at $\sim$ 510 cm^{-1}, suggesting that the 510 cm^{-1} mode is related only to the Sb^+ implantation too. However, we cannot specifically attribute the 510 cm^{-1} peak to the local vibration mode of the Sb on Zn site in ZnO because similar signals have been also observed in Fe, Al and Ga doped ZnO films grown by PLD.[22] The 510-cm^{-1} peak was attributed to the silent $2B_1$ (L) second-order modes in the Raman spectra.[23] This scattering is induced by the breakdown of the translation symmetry of the lattice caused by defects or impurities either because of the dopant nature or because of the growth condition.[23] So, it is reasonable to observe this mode in our samples be-

cause of the disorder in our ZnO film, introduced by the implanted large size Sb^+ ions. Very recently, the 510-cm^{-1} mode was attributed to the Zn_i–O_i complex, which was confirmed by different experiments and theoretical calculation consistent with our hypothesis of Zn_i survival in Sb^+ implanted samples.[24] Keeping in mind that our annealing conditions may leadingly introduce oxygen interstitials (remember that we carried out the anneals in oxygen plasma, which is a oxygen rich condition), we may consistently conclude the 510-cm^{-1} mode in the high dose Sb^+ implanted samples is related to Zn_i–O_i. For the Xe^+ implanted samples or the low dose Sb^+ implanted samples, however, the absence of 510-cm^{-1} peak is because few Zn interstitials exist in the ZnO films after annealing.

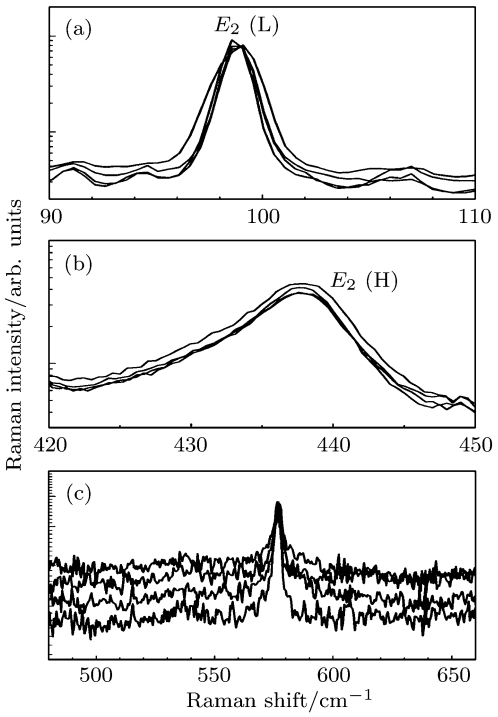


Fig. 3. Raman spectra of Xe^+ implanted ZnO after annealing and undoped ZnO relevant to E_2 (L) (a), E_2 (H) (b), and LO signatures (c).

Electrical measurement is employed in order to further investigate the difference in Zn_i concentration in Sb^+ and Xe^+ implanted samples between before and after annealing. Figure 4 shows the electron carrier concentrations measured in the annealed Sb^+ ion implanted samples. All samples are highly resistive before annealing because a great number of radiation-induced defects compensate the material (not shown). The trend observed in Fig. 4 may be interpreted in terms of increased concentration of Zn_i associated with Sb_{Zn}–$2V_{Zn}$ complex formation as discussed in Fig. 2. Consistently, much smaller variations in carrier concentration were observed in the samples implanted with Xe^+. Note that there is a significant carrier concentration drop in the annealed as-grown sample labeled with open symbol, which can be easily understood as the consequence of the introduction of O_i caused by the oxygen plasma annealing condition (compared with a value of $\sim 2 \times 10^{16}$ cm^{-3} of the as-grown sample). In contrast to Xe^+ implanted samples, the Sb_{Zn}–$2V_{Zn}$ complex acts as an acceptor in Sb^+ implanted ZnO as suggested from the theoretical calculations. However, there are formed even more Zn_i's associated with the Sb_{Zn}–$2V_{Zn}$ complex, which will lead to the n-type conduction, for Zn_i is a shallow donor in ZnO.[25] In our opinion, even we can obtain the Sb_{Zn}–$2V_{Zn}$ complex acceptor. It is difficult to achieve the p-type ZnO by ion implantation with large size Sb^+ because of the introduction of abundant shallow donors into ZnO simultaneously. However, we can realize the p-type doping in ZnO by *in-situ* Sb doping as reported previously,[9,10] where the shallow donor (Zn_i) could be eliminated by adjusting the growth conditions and parameters (such as the oxygen-rich growth condition).

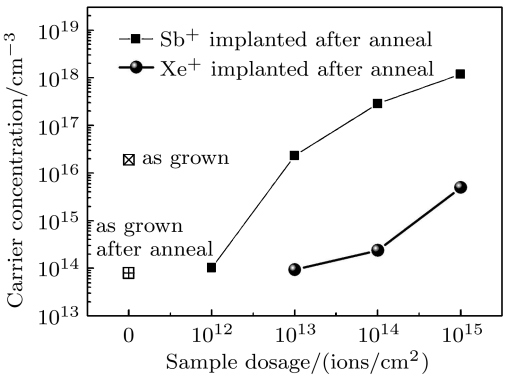


Fig. 4. Electrical measurements of as-grown undoped, as-grown after annealing and implanted ZnO after annealing.

4. Summary

We have investigated the correlation between the production of Sb–$2V_{Zn}$ complexes and Zn interstitials in ZnO epitaxial films before and after annealing by a combination of Raman spectroscopy and electrical measurements. The E_2 (H) modes are recovered totally in both Sb^+ and Xe^+ implanted samples after annealed in MBE chamber under the oxygen plasma protection. However, the unrecovered E_2 (L) modes of the high Sb^+ dose implanted samples suggest the damage of the Zn sublattice. The appearance of new

mode at 510 cm^{-1} only in the annealed high dose Sb^+ implanted sample is attributed to the Zn_i–O_i complex, which accords with the electrical measurement. The Sb_{Zn}–$2V_{Zn}$ complex acceptor is suggested to form in the Sb^+ implanted ZnO films after annealing, but all the samples are shown to be of n-type conduction, which may be explained in terms of compensation effect provided by Zn_i, a shallow donor in ZnO. However, p-type doping in ZnO can be realized by *in-situ* Sb doping in proper growth condition.

References

[1] Tang Z K, Wong G K L, Yu P, Kawasaki M, Ohtomo A, Koinuma H and Segawa Y 1998 *Appl. Phys. Lett.* **72** 3270

[2] Bagnall D M, Chen Y F, Zhu Z, Tao T, Koyama S, Shen M Y and Goto T 1997 *Appl. Phys. Lett.* **70** 2230

[3] Reynolds D C, Look D C, Jogai B, Litton C W, Cantwell G and Harsch W C 1999 *Phys. Rev.* B **60** 2340

[4] Neuvonen P T, Vines L, Kuznetsov A Yu, Svensson B G, Du X L, Tuomisto F and Hallén A 2009 *Appl. Phys. Lett.* **95** 242111

[5] Dunlop L, Kursumovic A and MacManus-Driscoll J L 2008 *Appl. Phys. Lett.* **93** 172111

[6] Wardle M G, Goss J P and Briddon P R 2005 *Phys. Rev.* B **71** 155205

[7] Janotti A and van de Walle C G 2007 *Phys. Rev.* B **76** 165202

[8] Park C H, Zhang S B and Wei S H 2002 *Phys. Rev.* B **66** 073202

[9] Mandalapu L J, Yang Z, Xiu F X, Zhao D T and Liu J L 2006 *Appl. Phys. Lett.* **88** 092103

[10] Chu S, Olmedo M, Yang Z, Kong J Y and Liu J L 2008 *Appl. Phys. Lett.* **93** 183106

[11] Limpijumnong S, Zhang S B, Wei S H and Park C H 2004 *Phys. Rev. Lett.* **92** 155504

[12] Wahl U, Correia J G, Mendonça T and Decoster S 2009 *Appl. Phys. Lett.* **94** 261901

[13] Gu Q L, Ling C C, Brauer G, Anwand W, Skorupa W, Hsu Y F, Djurisic A B, Zhu C Y, Fung S and Lu L W 2008 *Appl. Phys. Lett.* **92** 222109

[14] Braunstein G, Muraviev A, Saxena H, Dhere N, Richter V and Kalish R 2005 *Appl. Phys. Lett.* **87** 192103

[15] Wang X N, Wang Y, Mei Z X, Dong J, Zeng Z Q, Yuan H T, Zhang T C, Du X L, Jia J F, Xue Q K, Zhang X N, Zhang Z, Li Z F and Lu W 2007 *Appl. Phys. Lett.* **90** 151912

[16] Guo Y, Liu Y P, Li J Q, Zhang S L, Mei Z X and Du X L 2010 *Chin. Phys. Lett.* **27** 067203

[17] Özgür Ü, Alivov Y I, Liu C, Teke A, Reshchikov M A, Dogan S, Avrutin V, Cho S J and Morkoc H 2005 *J. Appl. Phys.* **98** 041301

[18] Ke X W, Shan F K, Park Y S, Wang Y J, Zhang W Z, Kang T W and Fu D J 2007 *Surf. Coat. Technol.* **201** 6797

[19] Artus L, Cusco R, Alarcon-Llado E, Gonzalez-Diaz G, Martil I, Jimenez J, Wang B and Callahan M 2007 *Appl. Phys. Lett.* **90** 181911

[20] Wang J B, Zhong H M, Li Z F and Lu W 2006 *Appl. Phys. Lett.* **88** 101913

[21] Cusco R, Jimenez J, Wang B and Callahan M J 2007 *Phys. Rev.* B **75** 165202

[22] Bundesmann C, Ashkenov N, Schubert M, Spemann D, Butz T, Kaidashev E M, Lorenz M and Grundmann M 2003 *Appl. Phys. Lett.* **83** 1974

[23] Manjón F J, Marí B, Serrano J and Romero A H 2005 *J. Appl. Phys.* **97** 053516

[24] Friedrich F, Gluba M A and Nicke N H 2009 *Appl. Phys. Lett.* **95** 141903

[25] Look D C, Hemsky J W and Sizelove J R 1999 *Phys. Rev. Lett.* **82** 2552